



PCCP

Electromagnetic Control of Spin-Ordered Mn³⁺ Qubits: A Density Functional Study

| | |
|-------------------------------|--|
| Journal: | <i>Physical Chemistry Chemical Physics</i> |
| Manuscript ID | CP-ART-08-2020-004455.R1 |
| Article Type: | Paper |
| Date Submitted by the Author: | 22-Sep-2020 |
| Complete List of Authors: | Hooshmand, Zahra; The University of Texas at El Paso, Physics Pederson, Mark; The University of Texas at El Paso, Physics |
| | |

SCHOLARONE™
Manuscripts

Electromagnetic Control of Spin Ordered Mn_3 Qubits: A Density Functional Study[†]

Zahra Hooshmand,^a and Mark R Pederson^{*a}

$[\text{Mn}_3\text{O}(\text{O}_2\text{CMe})(\text{dpd}_{3/2})]_2$ is composed of two monomers each of which contain three Mn atoms at the vertices of an equilateral triangle. A full analysis of the electronic and magnetic structure of the dimer shows that each Mn atom carries a local spin of $S=2$ while other spin states are energetically much higher. This result suggests application for conventional as well as quantum tasks. A detailed analysis of the electronic and magnetic structure of the monomer, on the other hand, suggests that there are three spin states of $S=1$, $S=3/2$ and $S=2$ per monomer which are energetically competitive. We found that while monomer-monomer interactions are very weak, the coupling of monomers via covalent linkers affects both the magnetization and electronic energy levels of monomers. In particular, the isolated monomers prefer a ground state with local spin of $S=1$ on Mn atoms and an antiferromagnetically ordered structure while the dimers possess a ground state with local spin of $S=2$ on Mn atoms and a ferromagnetically ordered structure. The investigation of the polarizability of both monomer and dimer is examined for antiferromagnetically ordered structures which induces a high dipole moment of 0.08 (a.u.) and 0.16 (a.u.) for monomer and dimer, respectively. The energy of the antiferromagnetic structure is also high compared to other spin-electric molecules.

^{0a} Department of Physics, University of Texas at El Paso, El Paso, Texas, 79968 USA.
E-mail: mrpederson@utep.edu

Electromagnetic Control of Spin Ordered Mn₃ Qubits: A Density Functional Study

September 21, 2020

1 Introduction

The "uncommon" properties of single molecular magnets put them on the forefront of the research on the materials for quantum and classical information storage. The superposition of several nearly degenerate ground eigenstates of these molecules leads to natural entanglement and the slow relaxation of their magnetization vector allows for enough time to complete a calculation without significant error. One of the seminal works on the application of SMMs for information storage is the work of Leuenberger and Loss where they showed that the Grover's algorithm can be used in molecular magnets with specific examples of Mn₁₂-acetate and Fe₈ SMMs¹. The application of SMMs not only facilitates the miniaturization of devices to the molecular scale, but also provides a limitless variety of these molecules since their structures can be tailored with atomic precision. Structurally, SMMs form crystals with hundreds of thousands of them in a typical sample. To have a single molecular magnet, the interaction between moieties should be very weak while the intramolecular interactions are the dominant factor in determining the magnetic structure. Each moiety is composed of spin carrying metal centers, *i.e.*, the total spin of the molecule is largely due to the localized spin on the metal atoms. The experimental methods to build independent SMMs in a crystal structure includes hydrogen-bonded and covalently linked supramolecular pairs². However the latter has advantage over the former since controlling the oligomerization of the coupled SMMs is difficult using hydrogen bonding. An example of SMMs synthesized through the use of covalent bonds between the linkers is Mn₃ dimer. The molecule consists of two Mn₃ SMM monomers³, that are covalently linked and form a SMM with a total spin of $S=12$, $S=6$ within each monomer, with Mn atoms carrying the +3 oxidation state, according to experimental results⁴. The experimental measurements confirm that the spins on the two SMMs are weakly coupled and imply that they maintain their intrinsic magnetic structure. Our results show that the monomer-monomer spin interactions are small but that the covalent connections do indeed change the magnetism of each monomer.

The structural properties of Mn₃ dimers (and monomers) are also important since Mn atoms form an equilateral triangle. The ground state (GS) of SMMs with similar structures is often composed of antiferromagnetically ordered spins. Such ordering results in spontaneous rearrangement of electric charge and formation of a permanent electric dipole moment within the triangle which allows for switching between quantum states

through applications of an external electric field, also known as the spin-electric effect^{5,6}. The experimental demonstration of this effect has only been recently reported for Cu₃⁷ and Fe₃⁸ SMMs. While for Cu₃, each Cu atom was reported to carry a spin of $S=1/2$, for Fe₃, the experimental data suggests a local spin of $S=5/2$.

The Goodenough-Kanamori rules provide a framework for understanding conditions under which a system prefers FM to AF behaviors for bridged metal-ions arrays on cubic lattices. Under such circumstances it is the relative symmetries, *i.e.* nodal structure, of neighboring d orbitals that determines FM or AF structure where these rules depend significantly on the fact that the local axes are not rotated relative to one another. While this assumption is not valid in triangular arrays, the fundamental principle that FM can arise when neighboring high-energy valence orbitals are automatically orthogonal in real space is still the proper means for qualitatively understanding FM vs AF coupling. An example can be provided by the recent realization that Fe-containing molecules, on triangular lattices, can exhibit multi-ferroic behavior and that such behavior may indeed result from qualitatively different bond angles⁹. Furthermore, Mn atoms in complexes are generally known to exhibit a diverse range of spin and charge states which suggests that the Mn₃ geometry could also have a richer diversity of low-energy magnetic structures. As in the cases of the Fe₃ molecule we have confirmed that there are indeed two qualitatively different Mn valences, with low and high spin respectively, that must be considered to fully understand the spin excitations⁹. The theoretical study of Johnson *et al.*⁹ shows that each Fe atom can have both high and low spin states with local moments of $S_{loc}=5/2$ and $S_{loc}=1/2$, respectively, both of which are energetically almost degenerate and therefore the molecule is a multiferroic qubit in which both spin states have a dipole moment that is large enough to be distinguished by an external electric field, with a more pronounced signature from high-spin moment due to larger dipole moment.

Motivated by these findings, we have performed DFT calculations on both the Mn₃ monomer and dimer SMMs. Mn₃ monomers and dimers are potentially useful quantum systems because there is experimental evidence that they either are, or with appropriate modification, can form equilateral triangles^{3,4}. For applications based on electrical switching induced by either spin-electric coupling in antiferromagnetic systems or magnetic switching based upon resonant tunneling of magnetization, a three-fold or higher symmetry axis is desirable, at least as a baseline, if

not required. As such a key component of the work discussed here is to perform our calculations subject to the constraint of a three-fold axis to determine if the Mn_3 system is expected to have perfect three-fold symmetry. The electronic and magnetic structures of each SMM have been studied and compared to both understand the properties of each individual monomer and dimer and to find the effect of monomers' pairing on the electronic and magnetic structure of dimers as well as monomers. Owing to its equilateral triangular structure, the possibility of an antiferromagnetically ordered SMM that gives a non-zero net dipole moment have also been studied. Moreover, we have calculated the total energy for different high and low spin states to examine the multiferroicity in both Mn_3 monomer and dimer structures.

The remainder of this paper is organized as follows. In section II we present an overview of the theoretical framework employed in this paper. We will discuss the calculation details for both structural optimization and spin interactions for calculations of exchange couplings. In section III the results and discussions on the magnetic and electronic structure are provided. Finally, in section IV we present the summary and conclusion of this study.

2 Methodology

2.1 Geometry Optimization

The structures of $[O(MnOOC_2H_3C_5H_4NCOR)_3]^{+1}$, ($R=H$ or CH_3) monomer and $[Mn_3O(O_2CMe)(dpd_{3/2})_2]^{+2}$ dimer are shown in Fig. 1. To obtain the monomer structure two terminations are possible: H and CH_3 . Our calculations show that both terminations give the same magnetic moments and the same HOMO-LUMO gap, as one can expect. The calculations performed in this paper have used the group symmetry. This helps with identification of structures that are not susceptible to Jahn Teller distortions and identifies structures that exhibit conventional resonant tunneling of magnetization. When aligned along the (111) axis, the point group of Mn_3 monomer can be generated from cyclic permutations of $(x,y,z) \rightarrow (z,x,y)$. The resulting group is of order three. There is no increase in efficiency associated with block-diagonalization of matrices into three complex irreducible representations. Instead we maintain real basis functions which allows for block-diagonalization into two reducible representations. The structure of Mn_3 monomer was made such that no sigma bonds were missing compared to the structure of Mn_3 dimer. To construct the structure of the dimer, another operation of $(x,y,z) \rightarrow (-z,-x,-y)$ was applied. This changes the order of group to six with a total of three representations of dimensions (1,1,2). The alignment of monomers with respect to one another in dimers results in a structure that is nearly eclipsed but neither perfectly staggered nor eclipsed. Using the symmetries mentioned above, the atomic structure of Mn_3 monomer and dimer was found to have 23 and 24 inequivalent atoms, respectively. Cartesian coordinates with full precision are available upon request.

The optimizations were done by performing density-functional

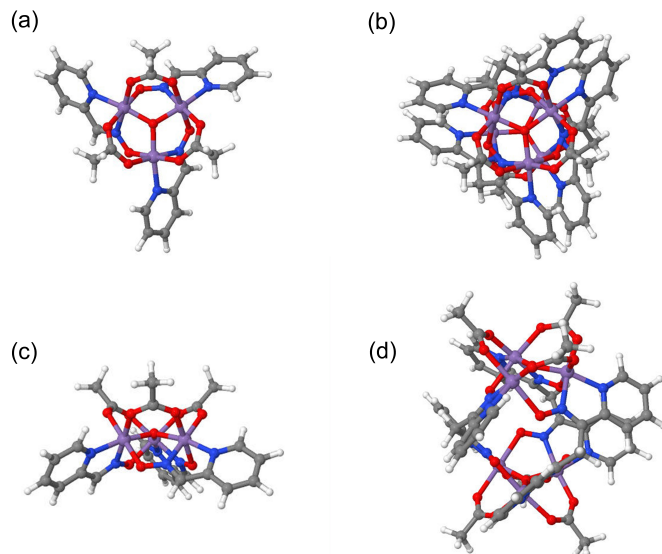


Figure 1 Top (a,b) and side (c,d) view of Mn_3 monomer and dimer molecular structures, respectively. The dimer is formed from two monomers of Mn_3 that are neither completely eclipsed, nor staggered. Color code of atoms: H:White, C: Dark grey, N: Blue, O: Red and Mn: Purple. The results of monomer calculations shows no difference between the H and methyl termination.

theory (DFT)^{10,11} calculations as employed in NRLMOL^{12,13} code. For both exchange and correlation interactions, the generalized-gradient approximation of Perdew-Burke-Ernzerhof¹⁴ was used. The Kohn-Sham orbitals were represented by Gaussian orbitals and the all-electron potential was used throughout the calculations¹⁵. The Limited memory Broyden-Fletcher-Goldfarb-Shanno (LBFGS) scheme programmed by Liu and Nocedal¹⁶ has been used for geometrical optimization. All the atoms were allowed to move until the forces acting on each atom in all directions were smaller than 0.001 Hartree/bohr with an energy convergence criteria of 0.000001 Hartree. For the Mn atom, 20 bare Gaussians with exponents varying from 0.04162- 0.35849×10^7 were used to construct a contracted basis set composed of 7 s-type, 5 p-type, and 4 d-type contracted orbitals. We will refer to this as $[Mn(5):0.04162-0.35849 \times 10^7, 7s5p4d]$. For the other atoms within this notation the basis sets are designed as: $[O(13):0.10492-0.61210 \times 10^5, 5s4p3d]$, $[N(13):0.09411-0.51751 \times 10^5, 5s4p3d]$, $[C(12):0.07721-0.22213 \times 10^5, 5s4p3d]$, and $[H(6):0.22838-0.77840 \times 10^2, 4s3p1d]$ ¹⁷. The spin-orbit interactions were turned on for all the spin-configurations. Four different spin states were examined by fully optimizing the Mn_3 monomer and dimer structures with local spin moments of $S_{loc} = 5/2, 2, 3/2$ and 1. The magnetic moment of each atom was calculated as the total spin polarization inside a sphere that is centered around that atom. This was done by capturing charge and spin within a sphere of radius 2.23, 1.45, 1.32, 1.25 and 0.57 bohr centered about Mn, C, N, O and H atoms, respectively. All the calculations corresponding to high and low spin states were performed in fixed moment mode. The coordinates, charge and magnetic moment of optimized monomer and dimer for the

most stable spin ordering are listed in Table 1.

2.2 Spin Hamiltonian

Assuming the orbitals in a partially filled shell remain the same when the local axis of quantization is flipped and in the absence of an external magnetic field the spin-spin interactions can be described using the following Hamiltonian:

$$H = \sum_{ij} J_{ij} \mathbf{s}_i \cdot \mathbf{s}_j \quad (1)$$

This Hamiltonian is also known as the isotropic or Heisenberg Hamiltonian. J_{ij} are the exchange parameters and \mathbf{s}_i and \mathbf{s}_j are the spins of magnetic atoms (i,j) in the SMM structure. This Hamiltonian is only correct for systems with localized spin moment. In section III, We will show how application of symmetries simplifies the solution to this equation. We will also validate the accuracy of our results by showing the localization of magnetic moment on the magnetic atoms only.

Another contribution to the spin Hamiltonian comes from the spin-orbit interaction. The effect comes from the motion of a charged particle with its magnetic dipole in the electrostatic field of ion's potential. The main effect of spin-orbit interactions is to shift the degeneracy of the spin multiplets of the GS. For systems with a finite gap, the first order correction is zero and the second order correction can be described by the following Hamiltonian:

$$H = DS_z^2 + E(S_x^2 - S_y^2) \quad (2)$$

Since we are working with a system which has three-fold axis, E is zero if there are no defects such as different isotopes or disordered molecules. If $D < 0$, the molecule is easy-axis and if $D > 0$, it is easy plane (that is perpendicular to z-axis). The parameter D can be extracted from DFT calculations. Within NRLMOL, this is done based on the perturbative method and checked through exact diagonalization. The details of this method can be found in Refs^{18,19}.

3 Results and Discussions

3.1 Electronic structure of Mn₃ Monomer and Dimer

Two identical Mn₃ monomers can be made by removing three C atoms from the dimer structure at a cost of 1.95 eV per C atom. As shown in Table 2, the Mn₃ monomer can exist in a less common low spin ($3d^{\uparrow\uparrow\uparrow\downarrow}$) and two more common high spin ($3d^{\uparrow\uparrow\uparrow}$, $3d^{\uparrow\uparrow}$) states. These spin states are equivalent to a local spin of $S=1$, $S=2$ and $S=3/2$, respectively. The Mn atom is known to rarely exist in a +5 oxidation state which could also provide a local moment of $S_{loc}=1$. Our calculations affirm that the $S_{loc}=1$ are due to single-electron spin-flips in the +3 oxidation state. For the $S_{loc}=1$ state, the configuration exhibits a nearly metallic behavior (HOMO/LUMO gap = 0.43 eV) while for $S_{loc}=2$ the configuration presents itself with a healthy gap (HOMO/LUMO gap = 0.75 eV). While the total energy difference between different spin states is rather small, with the smallest between $S_{loc}=1$ and $S_{loc}=2$, the magnetic anisotropy

Hamiltonian is qualitatively different for the three monomeric electronic configurations which should provide a means for identifying these competing phases as well as a means for using such behavior in a device or chemical sensing applications. For example, the $S_{loc}=1$ monomeric structure exhibits easy-axis behavior with a magnetic anisotropy difference of 10.49 K while $S_{loc}=2$ exhibit easy-axis behavior with magnetic anisotropy difference of 3.82 K. The explanation of why splitting the dimer into two reduces the moment per monomer by a factor of two is not entirely straightforward. However, it is entirely consistent with the multi-ferroic behavior that was observed recently in the Fe₃ trimer⁹. For that case it was observed that the $S=5/2$ Fe center ($d^{\uparrow\uparrow\uparrow\uparrow}$) was only slightly more stable than the $S=1/2$ ($d^{\uparrow\uparrow\uparrow\downarrow}$) even though one would expect a very large exchange splitting in the separated ion. What is clear is that an analysis of the dipole moments (larger for the $S=6$ monomers) are qualitatively different for the two spin states. This suggest that electrostatic potential on one monomer may affect the ordering of electronic states on neighboring monomers and is likely to be the cause for changes in the total moment of the ground state structures. However, a simple back-of-the-envelope estimation in changes in energies due to changes in long-range interactions between two monomers does not suggest that this is the origin in the change of moment.

For the Mn₃ dimer the different spin states are separated by bigger energy difference while still small enough for $S_{loc}=1$ and $S_{loc}=2$ to be considered as competitive in energy. The coupling between the two monomers results in the most stable structure with $S_{loc}=2$ and a HOMO/LUMO gap of 0.85 eV. Similar to the monomer, the dimer structure exhibits easy-axis behavior. However, compared to the most stable structure in the monomer, the magnetic anisotropy difference reduces to 6.88 K for the GS of dimer.

The analysis of electronic states of the most stable monomer structure shows that both HOMO and LUMO levels are spin minority states (Fig. 2). The HOMO and LUMO energy gap for spin majority state is 1.82 eV. The energy difference between the HOMO of minority and majority spin states is 0.75 eV. Our calculations show that this energy gap has 3 spin minority electrons. As a result of coupling between two monomers, the HOMO of the dimer changes from spin minority to spin majority while the LUMO remains spin minority. For minority spin state the HOMO-LUMO gap increases to 1.85 eV while for the spin majority states this gap reduces to 0.91 eV. The region between the HOMO of minority and HOMO of majority gives a forbidden energy interval of 1 eV for minority spins while there are 8 majority spin electrons in that energy region. As shown in Fig. 2, the states near Fermi level for both monomer and dimer structures are dominated by states coming from Mn atoms.

The magnetic moment on Mn atoms for both monomer and dimer SMMs were obtained to be at least two orders of magnitude larger than all the other atoms with a comparable moment on Mn atoms: 2.00 μ_B in monomer vs. 3.66 μ_B in dimer. The smaller magnetic moment of Mn atoms in the monomer is a direct result of a smaller spin state compared to the dimer. In Table 3, some bond lengths between atoms of the monomer and dimer in their

Table 1 The final coordinates of inequivalent atoms after optimization of the ferromagnetic Mn₃ monomer and dimer structures. Based on the symmetry operations on a ferromagnetically ordered structure, there is only one inequivalent Mn atom. The magnetic moment was obtained by integrating the net spin inside a sphere that is centered about each atom.

| Mn ₃ Monomer | | | | | |
|-------------------------|----------|----------|----------|----------------|--------------------|
| Atom ($M_s = 1$) | X (Bohr) | Y (Bohr) | Z (Bohr) | Charge (e) | Moment (μ_B) |
| Mn | 0.0616 | -3.4617 | 0.4229 | 23.6480 | -1.9712 |
| O1 | 3.8623 | -0.6615 | -2.2355 | 5.9031 | 0.0206 |
| O2 | -2.5810 | -4.1549 | 2.9133 | 5.9675 | -0.0072 |
| O3 | 0.0000 | 0.0000 | 1.0222 | 5.9211 | -0.1024 |
| O4 | 2.6888 | -3.8615 | 3.0953 | 5.9715 | -0.0092 |
| N1 | 0.4750 | -6.9776 | -0.9286 | 5.1429 | 0.0122 |
| N2 | 2.7625 | -2.8935 | -1.9985 | 5.1069 | 0.0451 |
| C1 | 3.4448 | -4.8033 | -3.4391 | 4.5560 | -0.0127 |
| C2 | 2.1569 | -7.1226 | -2.9072 | 4.5346 | 0.0100 |
| C3 | -4.2853 | -2.6639 | 3.7834 | 4.5470 | -0.0025 |
| C4 | 2.5308 | -9.3922 | -4.2246 | 4.5299 | -0.0066 |
| C5 | -0.8011 | -9.0686 | -0.2330 | 4.5195 | 0.0036 |
| C6 | 1.2005 | -11.5322 | -3.4983 | 4.5108 | 0.0105 |
| C7 | -0.4843 | -11.3670 | -1.4538 | 4.5209 | -0.0052 |
| C8 | -5.9400 | -3.7153 | 5.8580 | 4.5175 | 0.0027 |
| H1 | 4.8963 | -4.5990 | -4.8854 | 0.1670 | 0.0003 |
| H2 | 3.8520 | -9.4384 | -5.8058 | 0.1693 | -0.0001 |
| H3 | -2.1066 | -8.8396 | 1.3486 | 0.1648 | 0.0000 |
| H4 | 1.4588 | -13.3111 | -4.4998 | 0.1651 | 0.0001 |
| H5 | -1.5571 | -13.0043 | -0.8280 | 0.1629 | 0.0000 |
| H6 | -7.8045 | -2.8186 | 5.8435 | 0.1682 | 0.0001 |
| H7 | -5.0452 | -3.3271 | 7.6934 | 0.1654 | 0.0000 |
| H8 | -6.1122 | -5.7680 | 5.6623 | 0.1639 | -0.0001 |
| Mn ₃ Dimer | | | | | |
| Atom ($M_s = 2$) | X (Bohr) | Y (Bohr) | Z (Bohr) | Charge (e) | Moment (μ_B) |
| Mn | 4.0684 | 5.5038 | 0.6872 | 23.4237 | -3.6644 |
| O1 | 5.1335 | 0.1076 | -0.0945 | 5.9110 | -0.0014 |
| O2 | 3.5734 | 8.8482 | 2.0849 | 5.9769 | -0.0158 |
| O3 | 3.6707 | 3.6707 | 3.6707 | 5.9312 | -0.0762 |
| O4 | 8.0482 | 5.5199 | 1.1340 | 5.9792 | -0.0539 |
| N1 | 3.9409 | 6.7374 | -3.0179 | 5.1515 | 0.0060 |
| N2 | 4.5972 | 2.1916 | -1.2522 | 5.1276 | 0.0376 |
| C1 | 4.5701 | 2.3180 | -3.7303 | 4.5291 | -0.0151 |
| C2 | 5.2424 | 0.0000 | -5.2424 | 4.5043 | 0.0030 |
| C3 | 4.0632 | 4.8306 | -4.7617 | 4.5117 | -0.0064 |
| C4 | 2.3483 | 9.5105 | 4.0910 | 4.5600 | -0.0164 |
| C5 | 3.7278 | 5.3961 | -7.3330 | 4.5282 | -0.0005 |
| C6 | 3.5270 | 9.1352 | -3.7113 | 4.5279 | -0.0092 |
| C7 | 3.3040 | 7.8818 | -8.0538 | 4.5140 | -0.0072 |
| C8 | 3.2136 | 9.8039 | -6.2372 | 4.5308 | -0.0007 |
| C9 | 2.4682 | 12.2673 | 4.7044 | 4.5338 | -0.0021 |
| H1 | 4.9577 | 0.4016 | -7.2597 | 0.1665 | -0.0004 |
| H2 | 3.7791 | 3.8811 | -8.7283 | 0.1672 | 0.0000 |
| H3 | 3.4606 | 10.5069 | -2.1720 | 0.1666 | 0.0001 |
| H4 | 3.0262 | 8.3379 | -10.0442 | 0.1676 | 0.0001 |
| H5 | 2.9148 | 11.7689 | -6.7313 | 0.1679 | 0.0000 |
| H6 | 0.7887 | 12.8271 | 5.7622 | 0.1671 | 0.0000 |
| H7 | 4.1460 | 12.5777 | 5.8834 | 0.1641 | -0.0002 |
| H8 | 2.6944 | 13.3599 | 2.9667 | 0.1673 | -0.0002 |

ground states are presented.

Table 2 Energy differences between different spin states in Mn₃ monomer and dimer. Zero corresponds to the spin state with the lowest energy. As noted in text the dimer is lower in energy by 5 eV as a result of having three extra C atoms.

| Mn ₃ Monomer | | Mn ₃ Dimer | |
|-------------------------|----------------|-----------------------|----------------|
| S | ΔE(Total) (eV) | S | ΔE(Total) (eV) |
| 3 | 0.00 | 6 | 0.64 |
| 9/2 | 0.75 | 9 | 1.22 |
| 6 | 0.27 | 12 | 0.00 |
| 15/2 | 3.40 | 15 | 5.45 |

Table 3 Some bond lengths between atoms in the Mn₃ monomer and dimer structures. For comparison with experimental data, the same bond lengths are listed from Ref [3,4]. The experimental values for monomer from Ref [3], are that of structure 4 which is the closest to the monomer structure in this study. The numbers in parenthesis represent the S=3 state of the monomer as found in this study. Mn-O²⁻ is the distance between Mn atoms with central O atom within each monomer. carb = carboxylate, ox = oximate and py = pyridyl. All the numbers are in Angstrom.

| | Mn ₃ Monomer | |
|--------------------|-------------------------|------------|
| | This work | Ref[3] |
| Mn...Mn | 3.26 (3.17) | 3.20, 3.19 |
| Mn-O ²⁻ | 1.90 (1.86) | 1.87 |
| Mn-O (carb) | 2.10, 2.00 (1.95, 1.99) | 1.92, 2.18 |
| Mn-O (ox) | 2.19 (1.97) | 2.17 |
| Mn-N (ox) | 2.10 (1.94) | 2.008 |
| Mn-N (py) | 2.11 (2.01) | 2.02 |
| | Mn ₃ Dimer | |
| | This work | Ref[4] |
| Mn...Mn | 3.20 | 3.21 |
| Mn-O ²⁻ | 1.87 | 1.86 |
| Mn-O (carb) | 1.94, 2.20 | 1.94, 2.21 |
| Mn-O (ox) | 2.17 | 2.22 |
| Mn-N (ox) | 2.01 | 2.05 |
| Mn-N (py) | 2.03 | 2.07 |

3.2 Calculations of Exchange Couplings

From the results of magnetic moment, as listed in Table 1, we can simplify the solution of the spin Hamiltonian to the one for only Mn atoms. The calculations of exchange couplings is generally performed by calculating the energy of ferromagnetically (E^{FM}) and antiferromagnetically (E^{AF}) ordered states. The exchange coupling is then proportional to the energy difference between the two states. For Mn₃ monomer, this constant can be obtained using the following equations:

$$E^{FM} = E_0 + 3JS^2, \quad (3)$$

$$E^{AF} = E_0 - JS^2, \quad (4)$$

The calculations of exchange couplings are slightly different for Mn₃ dimers. Regarding the structure of Mn₃ dimer, two antiferromagnetic orderings are possible: (a) The spin on Mn atoms within each monomer are ferromagnetically ordered while the two monomers are antiferromagnetically ordered (AF1 structure), (b) The spin on Mn atoms within each monomer are antiferromagnetically ordered which results in frustrated spin configurations similar to antiferromagnetic structure of Mn₃ monomer, and the two monomers are ferromagnetically coupled (AF2 structure). These AF configurations are displayed in Fig. 3(b) and 3(c). Therefore three different J values should be calculated: J_{pp} , $J_{pp'}$, J_{ip} , which respectively correspond to plane-to-plane exchange coupling between the two nearest Mn atoms in two triangular planes, plane-to-plane exchange coupling between the next nearest Mn atoms in two triangular planes and in-plane exchange coupling between two Mn atoms within each monomer. Similar to the assumption of the equilateral triangle in monomer, only one in-plane exchange constant is considered between Mn atoms within each monomer. The exchange constants are then extracted by solving the following three equations.

$$E^{FM} = E_0 + 6J_{ip}S^2 + 3J_{pp}S^2 + 6J_{pp'}S^2 \quad (5)$$

$$E^{AF1} = E_0 + 6J_{ip}S^2 - 3J_{pp}S^2 - 6J_{pp'}S^2 \quad (6)$$

$$E^{AF2} = E_0 - 2J_{ip}S^2 + 3J_{pp}S^2 - 2J_{pp'}S^2 \quad (7)$$

From the above equations (eqs. 3 and 4), an apparently large exchange coupling parameter is extracted in monomer (See Table 4). However interpretation of the large AF-FM energy separation is complicated. For our calculations on AF-ordered monomer units, we observe a reproducible re-ordering of the d-orbital filling on a pair of Mn centers with anti-parallel alignment. In coincidence with this effect is the appearance of an induced electrical dipole (0.08 a.u.=0.20 Debye). A detailed analysis of the magnetic moments on the monomer in S=6 structure, shows that upon flipping of spin on one of the Mn atoms, the perfectly triangular structure reduces to an isosceles triangle with magnetic moment on Mn atoms as: -3.71, 3.49 and -3.47. The negative sign in the moment is to indicate the opposite direction of the spins of the Mn atoms with the third one. The results of exchange coupling parameters for the dimer are in excellent agreement with experimental values⁴. We also found a weak ferromagnetic coupling between monomers in the dimer structure which is in accord with experimental results⁴. For magnetic moments, a similar result was found for the dimer structure with S=12. The moments were obtained as -3.61, 3.44 and -3.48 confirming that rather than having a perfectly triangular symmetry the dimers also exhibit an isosceles triangular structure as was predicted for both monomer and dimer experimentally^{3,4}. For S=3 monomer structure, on the other hand, we found that the structure remains as an equilateral triangle upon flipping the spin on one of the Mn atoms with magnetic moments obtained as -1.95, 1.96 and -1.95. This finding shows that the low spin state of Mn₃ monomer with its AF ground state is a perfect candidate for spin electric effect. The potential for modulation of electric dipole exhibited by the monomer and its relatively open

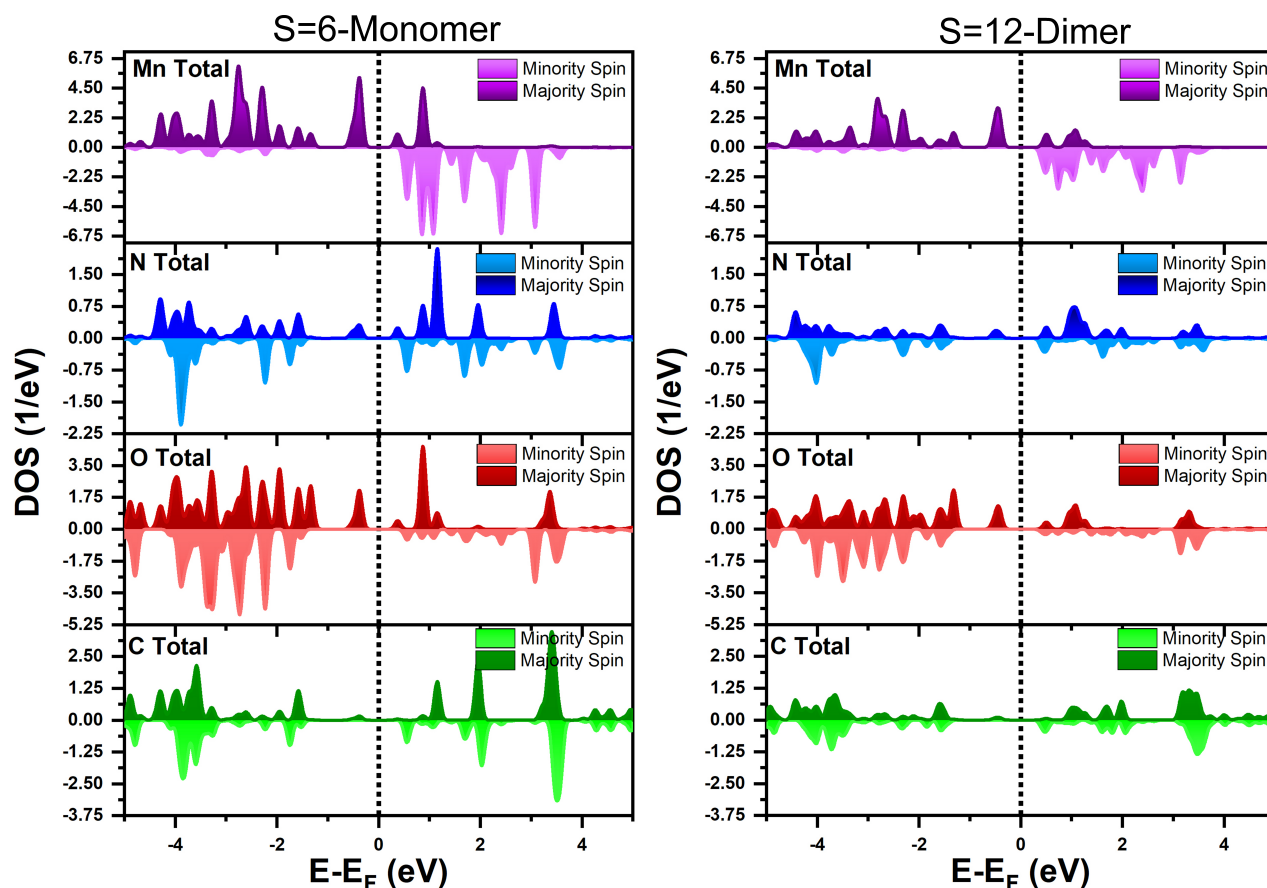


Figure 2 Atom projected total density of states of Mn_3 monomer for $S_{tot}=3$ and dimer for $S_{tot}=12$. The Fermi energy is set to the middle of HOMO and LUMO energies.

Table 4 Characteristic electronic and magnetic quantities of ground state of Mn_3 monomer and dimer. Magnetic anisotropy energies (MAE) were calculated using equation (2). The energy difference between FM and AF spin orderings were used to calculate exchange couplings. A negative energy difference indicates that AF structure is lower in energy. The value of exchange coupling in the dimer is only reported for in-plane interactions. We found that plane-to-plane interaction is three orders of magnitude smaller than in-plane interaction. The theoretical values in this table are obtained by adapting the convention in Ref [3,4]. For comparison, the MAE of the $S=3$ Mn_3 -Anion system is 1.4 K. The numbers with asterisk are experimental values from Ref [4]. For the dimer we found the D parameter to be 0.20 cm^{-1} which is comparable to 0.24 cm^{-1} of Ref [4]. Higher order contributions of the anisotropy Hamiltonian decrease the barrier as shown in the table.

| Mn ₃ Monomer | | | | | | |
|-------------------------|---------------------------------|---------|------------------------------|------------------------------|------------------|-------------------|
| S_{total} | $\Delta(\text{HOMO/LUMO})$ (eV) | MAE (K) | $\Delta(\text{AF/FM})$ (eV) | AF dipole (a.u.) | J (eV) | |
| 3 | 0.43 | 10.49 | -0.10 | 0.08 | 0.013 | |
| Mn ₃ Dimer | | | | | | |
| S_{total} | $\Delta(\text{HOM/LUMO})$ (eV) | MAE (K) | $\Delta(\text{AF1/FM})$ (eV) | $\Delta(\text{AF2/FM})$ (eV) | AF dipole (a.u.) | J (eV) |
| 12 | 0.85 | 6.88 | 0.0003 | 0.16 | 0.16 | -0.003 -0.003* |

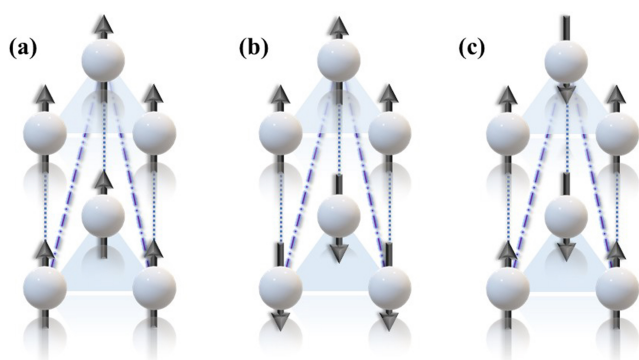


Figure 3 Schematic representation of antiferromagnetically ordered Mn_3 dimer. (a) Spins within each monomer are ferromagnetically ordered and coupled ferromagnetically to the next monomer (FM). (b) Spins within each monomer are ferromagnetically ordered and coupled antiferromagnetically to the next monomer (AF1). (c) Spins within each monomer are antiferromagnetically ordered which leads to frustrated spin order due to the triangular geometry of magnetic Mn ions (AF2). For visual purposes the Mn atoms within each monomer are shown as the vertices of equilateral triangles. In each figure the Mn_3 units are shown as vertices of the triangle. Dotted and dashed-dotted lines show J_{pp} and $J_{pp'}$ interactions. For visualization purposes, only one dashed-dotted line is shown.

structure, which appears to have funnel-shaped units that could trap anions, suggests the possibility of a cationic monomer (Mn_3) in close proximity to a symmetry preserving anion (A) that, upon deposition, could provide an array of ordered Mn_3 -A molecular magnetic dipoles that would strongly respond to an applied axial electric field and open up the possibility for a voltage-controlled quantum device with classically switchable electric dipoles if not magnetic dipoles. To investigate this point we have performed model calculations on a Mn_3 -Perchlorate monomer molecule system (Fig. 4). For the docked structure the energy of the $S=6$ state is 2.48 eV above the $S=3$ state. The local charges and moments on the Mn atoms are 23.5/3.56 for the $S=6$ and 23.5/1.9 for the $S=3$ respectively. We interpret these results, along with other local charge analyses in this paper, to argue that $S=2$ to $S=1$ local spin transitions, on the Mn, are responsible for the overall high-spin low-spin transition and that charge transfer to the ligands is an unlikely mechanism. The local moments for the Mn_3^{+1} isolated molecule are given by 2.00 and 3.72 for the $S=3$ and $S=6$ structures, respectively which indicates that there will be a slight change in the magnetic moment of the monomers due to the presence of counterion. For dimer structures, on the other hand, the exchange coupling within monomers as well as between them is found to be very small. A similar analysis of the magnetic moments of the AF dimer (AF2 in particular) shows the same trends in the magnetic moments of the Mn centers and suggests the same re-ordering of the d-orbitals filling on the anti-parallel Mn atoms.

4 Summary and Conclusions

The results of DFT analysis on Mn_3 dimer shows that the molecule has a ferromagnetically ordered GS with $S=12$. Other states of Mn atom were also studied by performing fixed-moment

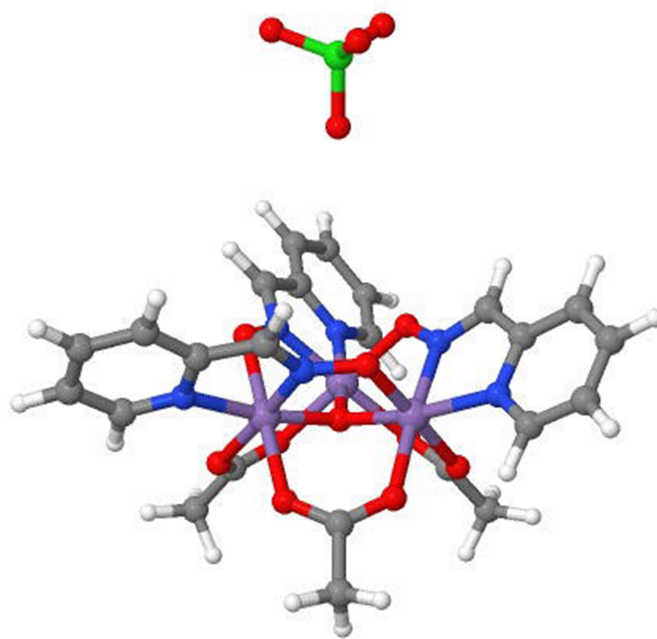


Figure 4 The structure of Mn_3 -Perchlorate monomer. Color code of atoms: H:White, C: Dark grey, N: Blue, O: Red, Mn: Purple and Cl: Green.

calculations for high and low spin states. The results of these calculations show the existence of two energetically competitive states in monomer ($S_{total}=3$ and $S_{total}=6$) and dimer ($S_{total}=6$ and $S_{total}=12$) which implies that the quest for a two-level quantum system could be realized from the anisotropy Hamiltonian but not from the Heisenberg Hamiltonian. The dipole moment of the frustrated spin orderings in both monomer and dimer are comparable to the results obtained for Fe_3 ⁹ and suggests a strong spin-electric effect. A comparison between the electronic and magnetic structures of a single Mn_3 monomer with Mn_3 dimer, shows that not only the covalent linkers affect the electronic structures of the majority and minority spin states, but also the magnetization of Mn atoms is affected due to different local spin moment of isolated and dimerized monomers. Moreover, our calculations show that the GS of dimer changes to FM ordered structure while the monomer prefers an AF structure. When the effect of counterion is accounted, the GS magnetic structure of monomer changes and the energy ordering between the FM and AF structures is converted. This implies that counterion changes the electronic structure of monomer and will possibly have similar effects on the dimer. The details of this change will be the subject of a separate paper.

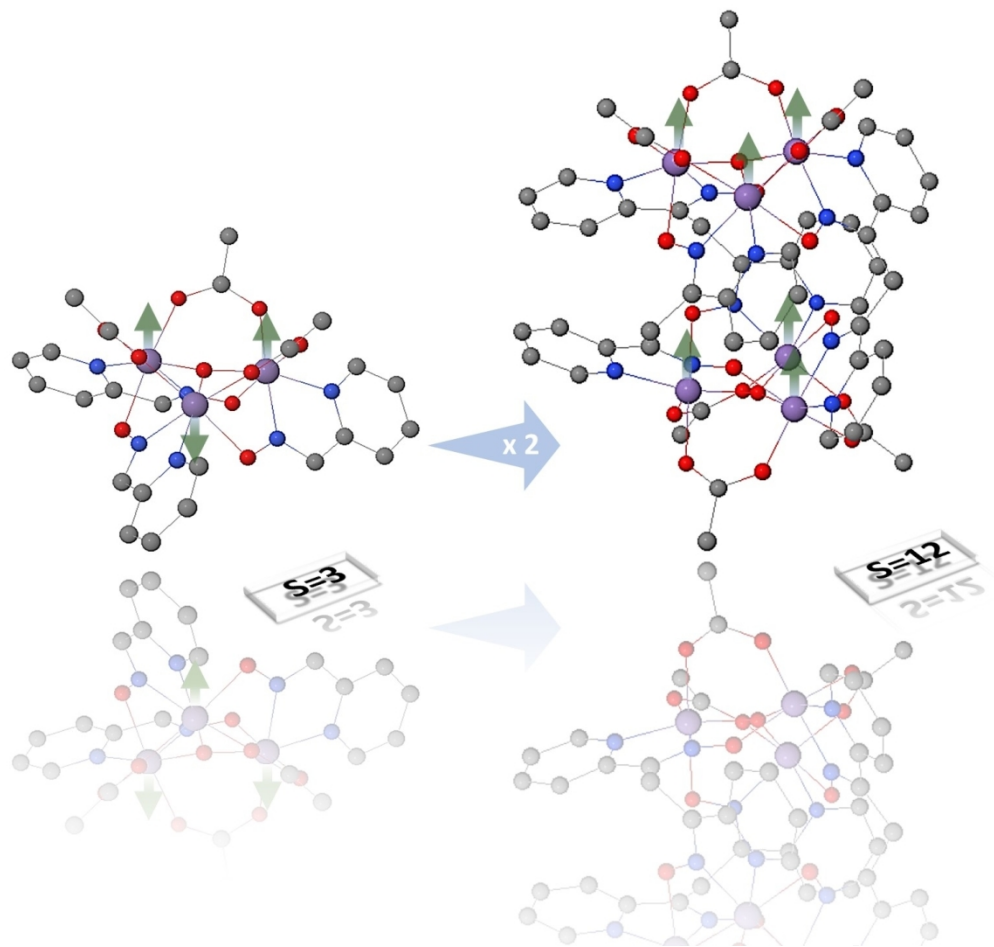
5 Acknowledgements

The calculations of this study were performed on XSEDE and NERSC supercomputers. This work was supported from startup funds provided by the University of Texas-El Paso and the Texas Science and Technology Acquisition and Retention (STARS) program and by the M²QM Energy Frontier Research Center under

grant DE-SC0019330.

Notes and references

- [1] M. N. Leuenberger and D. Loss, *Nature*, 2001, **410**, 789–793.
- [2] S. Hill, R. Edwards, N. Aliaga-Alcalde and G. Christou, *Science*, 2003, **302**, 1015–1018.
- [3] T. C. Stamatatos, D. Foguet-Albiol, S.-C. Lee, C. C. Stoumpos, C. P. Raptopoulou, A. Terzis, W. Wernsdorfer, S. O. Hill, S. P. Perlepes and G. Christou, *Journal of the American Chemical Society*, 2007, **129**, 9484–9499.
- [4] T. N. Nguyen, M. Shiddiq, T. Ghosh, K. A. Abboud, S. Hill and G. Christou, *Journal of the American Chemical Society*, 2015, **137**, 7160–7168.
- [5] D. Khomskii, *Nature communications*, 2012, **3**, 1–5.
- [6] J. Liu, J. Mrozek, W. K. Myers, G. A. Timco, R. E. Winpenny, B. Kintzel, W. Plass and A. Ardavan, *Physical review letters*, 2019, **122**, 037202.
- [7] B. Kintzel, M. Böhme, J. Liu, A. Burkhardt, J. Mrozek, A. Buchholz, A. Ardavan and W. Plass, *Chemical communications*, 2018, **54**, 12934–12937.
- [8] A. K. Boudalis, J. Robert and P. Turek, *Chemistry—A European Journal*, 2018, **24**, 14896–14900.
- [9] A. I. Johnson, F. Islam, C. M. Canali and M. R. Pederson, *The Journal of chemical physics*, 2019, **151**, 174105.
- [10] Y. Wang and J. P. Perdew, *Physical Review B*, 1991, **43**, 8911.
- [11] J. P. Perdew, J. A. Chevary, S. H. Vosko, K. A. Jackson, M. R. Pederson, D. J. Singh and C. Fiolhais, *Physical review B*, 1992, **46**, 6671.
- [12] M. R. Pederson and K. A. Jackson, *Physical Review B*, 1990, **41**, 7453.
- [13] K. Jackson and M. R. Pederson, *Physical Review B*, 1990, **42**, 3276.
- [14] J. P. Perdew, K. Burke and M. Ernzerhof, *Physical review letters*, 1996, **77**, 3865.
- [15] D. Porezag and M. R. Pederson, *Physical Review A*, 1999, **60**, 2840.
- [16] D. C. Liu and J. Nocedal, *Mathematical programming*, 1989, **45**, 503–528.
- [17] D. Porezag and M. R. Pederson, *Phys. Rev. A*, 1999, **60**, 2840–2847.
- [18] M. Pederson and S. Khanna, *Physical Review B*, 1999, **60**, 9566.
- [19] M. Pederson and S. Khanna, *Chemical Physics Letters*, 1999, **307**, 253 – 258.



406x406mm (96 x 96 DPI)